Optical-Layer Routing Influence on Software-Defined C-RAN Survivability

Houman Rastegarfar, Tommy Svensson, and Nasser Peyghambarian

***Abstract*—The cloud radio access network (C-RAN) architecture based on heterogeneous radio resources and centralized processing holds promise for satisfying the diverse requirements of fifth-generation (5G) mobile applications. In order to provide fronthaul/backhaul connectivity to the radio resources, not only does a dynamic software-defined networking (SDN) optical transport (X-haul) solution resolve the capacity scaling bottlenecks, but it can also lead to statistical multiplexing gains and power efficiency in the system. Infrastructure programmability due to SDN, however, can result in network reliability concerns due to the inherent cyber-physical interdependency between the physical fiber and the higher-layer (IP) control networks. In this paper, we study the SDN C-RAN robustness to node failures, considering the interplay of wireless, optical, and control domains, and examine the effectiveness of two optical-layer routing mechanisms, i.e., static load balancing and dynamic routing, for survivable system operation. Our Monte Carlo analysis points to the marginal advantage of load balancing, irrespective of connection distribution in the control plane. However, optical X-haul programmability provides for robust C-RAN operation with essentially no sensitivity to critical network elements and negligible penalty in terms of fronthaul segment latency.**

***Index Terms*—Cloud radio access network (C-RAN), infrastructure programmability, load balancing, routing, software-defined networking (SDN), survivability.**

I. Introduction

THE fifth generation of cellular networks (5G), to be rolled out by 2020, is emerging to address the disparate requirements of a myriad of services and applications. New technologies and use cases such as the Internet of Things (IoT), smart city infrastructure, ultrahigh resolution video streaming, tactile Internet, road safety and autonomous vehicles, wearable devices, and augmented reality introduce new quality of service (QoS) requirements and the need for dramatic performance enhancements in terms of throughput, end-to-end latency, and reliability. Compared to the existing cellular systems, the key performance indicators of 5G networks imply 1,000 times higher traffic rates, up to 100 times more connections, millisecond-scale end-to-end latencies, and up to 10 Gb/s stationary access rates [1]–[6]. These drastic improvements call for innovations across multiple technology domains, including the densification of wireless access points in new network architectures, the use of new frequency bands in the wireless domain, massive multiple-input, multiple-output (mMIMO) and advanced signal processing schemes, new control solutions based on software-defined networking (SDN), and network function virtualization (NFV) [5]–[11].

From a radio network architecture perspective, two major trends are expected to bring about improvements in the system performance: 1) the densification of radio access points in a tiered heterogeneous network (HetNet), and 2) the centralization of baseband processing functions to improve radio coordination, system cost, and energy consumption. The former trend involves the introduction of small cells (SCs) along with legacy macro cells (MCs) for improved wireless coverage, and the latter is based on decoupling the radio and baseband processing functions in a centralized/cloud radio access architecture (C-RAN). In the C-RAN architecture, remote radio heads (RRHs) are connected to the pool of baseband processing resources as well as the evolved packet core (EPC) [12]. The multiplicity of the radio nodes, the high traffic rates, and the latency and capacity requirements imposed by coordination schemes and existing standards such as the Common Public Radio Interface (CPRI) protocol pose significant challenges to designing transport networks for interconnecting the fixed radio resources in a scalable fashion [12]–[19].

The immense capacity and power efficiency of transparent optical fiber networks makes them a promising candidate for fronthauling (connecting the RRHs to the baseband processing pool) and backhauling (connecting the baseband processing resources to the EPC) in C-RANs. While legacy optical networks have been widely static due to overprovisioning and the complexities of real-time or near real-time switching in the optical layer, 5G wireless applications require an optical transport (X-haul) solution that is highly scalable and dynamic to efficiently move the existing resources where they are needed [12], [20]. Otherwise, the cost of an overprovisioned static solution considering the explosion of traffic would be prohibitive. Fortunately, SDN in optical transmission systems is being introduced and standardized for on-demand wavelength services, i.e., the dynamic switching of highly variable traffic patterns directly in the optical domain. With proper abstraction schemes, it is possible to provide application programming interfaces (APIs) to higher layer control applications and services, exposing optical infrastructure capabilities to be dynamically programmed and virtualized [21]–[25]. In a C-RAN scenario, the optical SDN controller can be coupled with the radio SDN controller and orchestrated within a hierarchical control plane architecture for the joint optimization of radio and optical resources [12], [26], [27].

H. Rastegarfar and N. Peyghambarian are with the College of Optical Sciences, University of Arizona, 1630 E. University Boulevard, Tucson, Arizona 85721, USA (e-mail: rastegarfar@gmail.com).

T. Svensson is with the Department of Electrical Engineering, Chalmers University of Technology, 412 96 Gothenburg, Sweden (e-mail: tommy.svensson@chalmers.se).

This work was presented in part at the 2018 Optical Fiber Communications Conference (OFC).

Manuscript received April 8, 2018; revised July 25, 2018.

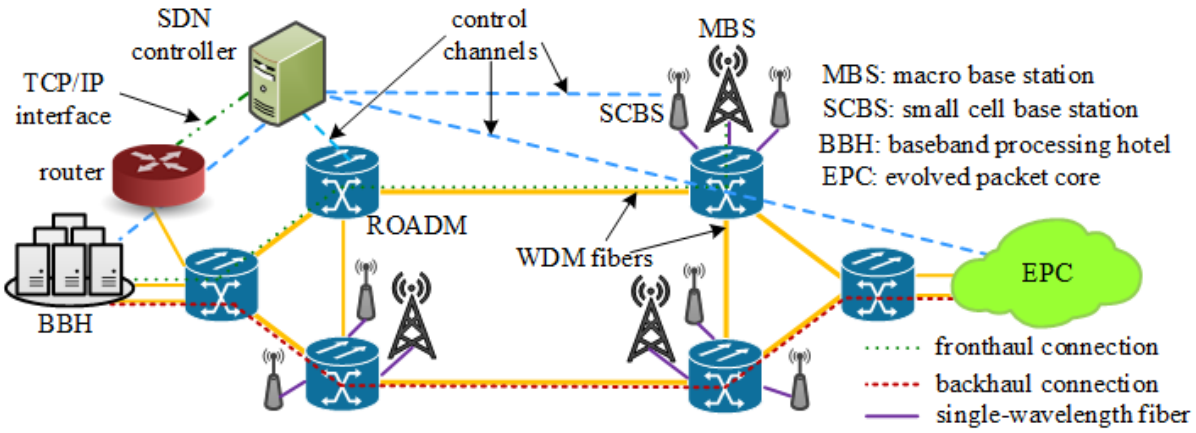

Fig. 1: Reference software-defined C-RAN architecture.

Although optical infrastructure programmability due to SDN leads to C-RAN resource usage efficiency and improved coordinated radio transmission, it makes the network failure response a significant issue. In software-defined optical transmission networks, a higher-layer, logically centralized controller disseminates IP control and signaling messages to the optical network hardware. On the other hand, the optical layer provides the control plane with the physical communication resources for its operation. This IP-optical layer interaction is indeed an example of cyber-physical interdependency [28]. Interdependent systems can be highly susceptible to failure events due to the cascade of failures between different domains, which in certain scenarios can result in a total outage [28]–[33]. As the software-defined C-RAN relies on a programmable optical transport network, it becomes crucial to assess its reliability from a network dependency perspective.

Unreliable X-haul operation is a significant issue from a cellular network performance point of view and has been shown to significantly diminish the performance gains offered by coordinated multipoint (CoMP) transmission techniques [34]. Research on optical X-haul reliability does exist [35]–[38]; however, the reliability implications of control and data plane topologies in an SDN framework are missing. While the cost advantages of dynamic resource sharing have recently been demonstrated in 5G transport networks [12], to the best of our knowledge, our earlier work in [38] is the only existing effort studying the impact of optical layer agility on SDN-enabled C-RAN robustness. Other existing works study the problem of survivability outside the context of control-data plane interactions and the dependencies among network entities. In Ref. [36], two avenues for enhanced reliability in 5G HetNets are investigated, namely, localized fiber-lean redundancy in the optical backhaul network and wireless bypassing of backhaul fiber faults. In Ref. [37], the authors study the problem of joint 5G optical transport survivability and power saving based on sleep mode operation.

The main novelty of this work is the deep survivability assessment of software-defined optical C-RANs in the context of cyber-physical interdependency, taking into account the topological properties at control and data plane levels. As the characteristics of a logical topology are determined by the network routing algorithm, we especially focus on the impact of optical-layer routing mechanisms. This paper extends our previous work in [38] by examining the possibility of robust C-RAN operation through load-balanced routing in an effort to introduce proactive protection in extreme conditions in addition to reactive optical layer restoration that is enabled by dynamic routing. Load balancing is primarily introduced with the goal of resolving the formation of critical path segments that are intrinsic to C-RANs due to the properties of fronthaul and backhaul connections. Compared to traditional optical protection/restoration techniques, with load balancing it is feasible to overcome both the penalties of additional backup hardware (for protection) and the hardware reconfiguration and rerouting latencies (for restoration). However, its effectiveness in SDN-enabled C-RAN has yet to be determined. To better understand the problem, we study the impact of the control plane in isolation whether or not load balancing is applied to its connections. Furthermore, we study the reliability implications of the hard limits that may be imposed on the fronthaul segment latency. Under a hard node failure scenario, our analysis points to the marginal advantage of load balancing compared with dynamic routing and calls for developments towards a fully programmable optical layer.

The rest of this paper is organized as follows. In Section II, we define our reference C-RAN architecture based on optical transport and unified SDN control. In Section III, we detail the dependencies among the radio, optical, and control domains, describe our failure model, and propose two solutions for counteracting the system sensitivity to the existing network dependencies and cascading failures; namely, load-balanced routing and dynamic routing. We study the failure response of wireless and optical networks in a 5G C-RAN scenario in Section IV, taking into account the effectiveness of the routing strategies in isolation as well as jointly. Finally, we summarize our findings and conclude in Section V.

II. Software-Defined Optical C-RAN Architecture

We consider a C-RAN based on a dense wavelength-division multiplexing (DWDM) reconfigurable optical add-drop multiplexer (ROADM) transport network. Fig. 1 depicts the network architecture, where the RRHs, supporting radio frequency (RF) functionalities, are separated from the baseband processing units (BBUs) that perform digital baseband processing. The BBUs are pooled into a centralized baseband processing hotel (BBH). In line with a heterogeneous network architecture, two types of RRHs are envisioned. Macro base stations (MBSs) are always active to provide coverage over the entire area, and small cell base stations (SCBSs) are provisioned for additional capacity on demand. Each ROADM node is assumed to provide fiber connectivity to its neighboring MBS and SCBSs.

In the reference architecture, each BBU port in the BBH and each RRH is equipped with a wavelength tunable transponder. The traffic from the wireless nodes (i.e., RRHs) neighboring a ROADM node is wavelength multiplexed and delivered to one of its port. For activating an RRH, two bidirectional connections should be set up in the optical transport network: one from the RRH to the BBH (i.e. fronthaul connection) and another from the BBH to the EPC (i.e. backhaul connection). While the fronthaul segment is characterized by high capacity and strict delay requirements, the traffic of a backhaul connection is packet based and of lower capacity. Hence, multiple backhaul connections can share a wavelength channel per an appropriate packet multiplexing technique. The total number of wavelengths required for carrying the traffic of the backhaul segment depends on the total aggregated backhaul traffic as well as the capacity per wavelength channel [12]. In our reference architecture, we assume all RRHs can connect to the provisioned BBH while satisfying the fronthaul latency constraints.

The operation of the optical C-RAN is governed by a logically centralized, omniscient SDN controller, which enables the optimization of the network performance through control applications. Due to the heterogeneity of the available resources, a hierarchical SDN control plane, comprising separate technology domain controllers can provide for the dynamic and joint optimization of radio, transport, and cloud resources [27]. In fact, the controller in Fig. 1 is made up of optical, wireless, and cloud controllers all interacting under a global orchestrator. While the centralized controller can actually be realized by incorporating multiple physical controllers at different locations of the network for reliability, scalability, and responsiveness [39]–[43], for examining the proposed solutions under *worst-case operating conditions*, we consider all the physical control hardware to interface one specific ROADM node using an IP router. The dash-double dotted line in Fig. 1 is the physical interface between the SDN control hardware and the router, and denotes the first (last) segment of outgoing (incoming) TCP/IP connections. We also assume the C-RAN to include only one BBH and one node interfacing the EPC and that the controller and the BBU resources to be co-located and connected to the same optical node (i.e., the BBH hub). The optical node interfacing the EPC is denoted as the EPC hub.

We can distinguish three network topologies in Fig. 1 that play an important role in determining the survivability of the optical C-RAN. The ROADMs and the fiber links interconnecting them form a "physical" network topology. The IP control connections and the fronthaul/backhaul connections form two "logical" topologies, i.e., logical control network and logical radio network topologies, respectively. The logical connections are mapped onto the physical fiber network through a routing and wavelength assignment algorithm. Here, we consider shortest-path routing with first-fit wavelength assignment.

III. Optical C-RAN Survivability and Routing Mechanisms

The reference C-RAN architecture in Fig. 1 is composed of three distinct network entities: 1) the radio access network comprising the RRHs and BBUs, 2) the optical X-haul network comprising ROADM nodes, fiber links, optical transceivers, amplifiers, etc., and 3) a higher layer (i.e., IP layer) SDN control plane responsible for controlling the wireless and optical network domains. In this study, we do not consider the power grid. However, in practice the power grid provides the network elements with power and receives control for its operation.

The operation of the C-RAN architecture depends on a programmable optical X-haul network, which introduces cyber-physical interdependency in the system [38]. This interdependency arises in highly dynamic software-defined optical transmission. In such a case, the physical fiber network elements (including ROADM nodes and optical amplifiers) rely on regular information exchanges with the higher-layer (i.e., cyber) SDN control plane for stable and optimal operation. On the other hand, the IP-based SDN control plane depends on the physical fiber network for the dissemination of its messages. This interdependency renders the C-RAN highly susceptible to failures, since a single failure in one domain can potentially trigger a series of failures across the domains and lead to cascading failures with significant consequences.

For assessing the reliability of an optical C-RAN, the dependencies among the constituent technology domains should be defined. Referring to the architecture in Fig. 1, Fig. 2 illustrates the existing dependencies in the system with arrows denoting the dependency direction. The IP-based SDN control plane provides control functionalities to both optical X-haul and radio access networks. Hence, these two networks depend on the SDN control plane for their operation. The SDN control messages are assumed to be disseminated over wired interfaces only. As a result, the control network depends on the optical network (hence, cyber-physical interdependency with potential for cascading failures). Finally, the RAN depends on the optical X-haul network for frontauling and backhauling the radio equipment. These four different dependencies denote the directions for the propagation of failures. For instance, a failure in either the control network or the X-haul network can lead to a failure scenario in the RAN. However, a failure event in the RAN will not affect the two other entities. In order to quantify

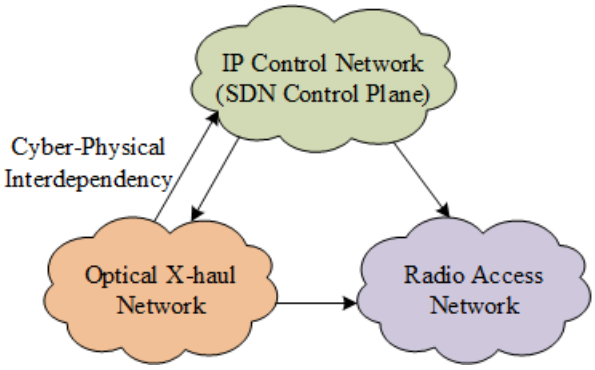

Fig. 2: Dependencies in the proposed software-defined C-RAN.

C-RAN reliability with regard to the functionalities provided by a reconfigurable optical X-haul network, we define our failure model as detailed by the following set of rules.

1) A physical node (either optical or wireless) fails when it loses connectivity to the controller.
2) A fiber link fails as soon as either of its neigboring ROADM nodes fails.
3) If a ROADM node fails, all RRHs directly connected to that node will fail since they lose connectivity to the X-haul network.
4) If a fronthaul or backhaul connection is lost, its corresponding wireless node (RRH) fails.
5) The ROADM node connecting to the SDN control hardware and the BBH (i.e., BBH hub) is highly protected and never fails. Otherwise, the whole system will be brought to a halt due to the lack of control signals. On the other hand, the EPC hub fails if it loses its connection to the control network.

This is a hard failure model in which a node fails when it loses connection to the controller. In practice, it is possible for a node to continue its static operation without higher layer control. A more relaxed, soft failure model as well as a model in which link failures replace node failures result in less severe performance degradation. However, in an effort to study the performance under harsh operating conditions (i.e., worst-case analysis), we assume the case where the lack of control results in physical-layer instability and an inevitable failure.

While the failure detection time by the SDN controller, controller response time, dynamics of the network protocol stack, hardware reconfiguration speeds, and traffic characteristics affect the network throughput, we hide these case-specific details in our abstract failure model in order to focus only on the topological properties of the SDN-enabled C-RAN. As a future step, this model should be extended to include the time aspect associated with the network elements and protocols.

We consider two possible mechanisms that can be implemented in the optical layer of the SDN-enabled C-RAN for improved survivability. The former technique is static load balancing in an effort to avoid single points of failures. The latter technique is the dynamic routing of connections based on rapid wavelength switching.

A. Optical-Layer Load Balancing

There exist three types of connections in the reference architecture of Fig. 1. Control connections contribute to the SDN control plane and form a connected logical topology on top of the physical fiber network. Through these connections, each optical or wireless node interfaces the SDN controller attached to the BBH hub. Fronthaul connections and backhaul connections are set up for connecting the RRHs to BBU resources and the EPC, respectively. The traffic rate of a backhaul connection is typically much lower than that of a fronthaul connection [12]; hence, the traffic from multiple backhaul connections can be properly aggregated and carried on a single wavelength. By default, shortest-path routing can be employed to map these connections onto the optical transport network. However, this could lead to unbalanced resource utilization, resulting in higher vulnerability wherever the concentration of connections is high.

Let $C_{N\times N}$ denote the physical cost matrix in an optical network of N ROADM nodes. $C(i,j) = C(j,i)$ is the cost associated with the bidirectional link connecting nodes i and j. If there is no direct fiber link between nodes i and j, $C(i,j) = 0$. If the cost of all fiber links is equal and fixed, then the problem of shortest-path routing reduces to minimum hop-count routing. With a static cost matrix, the connections are always mapped to the shortest path between a desired pair of source and destination nodes until wavelength blocking occurs and the next shortest path is considered. In a C-RAN architecture, this routing strategy could lead some links and nodes to be heavily loaded. For instance, each active RRH in Fig. 1 requires a backhaul connection from the BBH hub to the EPC hub. As long as the shortest path between these two hubs has capacity, backhaul connections will keep being mapped onto this path. As a result, the network elements on the path become highly critical, with a single failure resulting in total RAN outage.

When distributing the traffic over different routes (i.e., optical-layer load balancing), it is possible to improve the resilience of the RAN to single failure events. Not only load balancing can prevent the formation of a single point of failure, but it also enhances the delay/throughput performance of communication networks by resolving congestions, resulting in improved system scalability [44]. As it is possible to balance the connections upon their arrival, load balancing does not suffer from the deficiencies of traditional protection (in terms of dedicated backup hardware) and restoration (in terms of rerouting latency) techniques. However, compared with shortest-path routing, load balancing in a ROADM network leads to longer connections paths, which can be undesirable for delay-sensitive applications.

To perform load balancing in the optical X-haul network, the physical network cost matrix should be dynamically updated. We define aggregation coefficient, AC, as the ratio of frontaul connection bit rate to backhaul connection bit rate. Assuming that fronthaul and control connections are both allocated full wavelength capacity, the traffic of AC backhaul connections can be accommodated on a single wavelength. We define three routing mechanism as follows.

1) Routing R1: The cost matrix is static, with its nonzero entries being equal to 1. All connections are mapped onto the optical transport network based on minimum hop-count routing (i.e., baseline routing scheme, no load balancing).
2) Routing R2: The cost matrix is dynamic to perform load balancing. The default cost of any fiber link is equal to 1. For each connection mapped onto a fiber, the fiber cost is incremented by 1. Upon a connection release, the corresponding link cost is decremented by 1.
3) Routing R3: As in R2, the cost matrix is dynamic. However, the increment/decrement values depend on the connection type. If a backhaul connection (smallest-size connection) has to be mapped on a fiber, its cost is increased by 1. For fronthaul or control connections, the cost is increased by AC. Upon the release of a connection, the cost values are updated accordingly.

The following pseudocode of algorithm *CostUpdate()* illustrates the differences of R1, R2, and R3. The differentiating factor is how the physical cost matrix is updated upon a connection setup or teardown. Both R2 and R3 are strategies for implementing load balancing in the network. The former treats all connections equally, whereas the latter takes the bit rate disparities into account. These routing strategies do not depend on the reconfiguration capabilities of the physical layer and only come to action at the times of connection setup or release.

Algorithm CostUpdate(C, R, M, L, r)

Inputs: C indicates the physical cost matrix; R : routing mechanism; M : update mode (=1 for connection setup and -1 for connection teardown), L : ordered list including the nodes along the route from the source to the destination; r : required connection capacity ($\in \{1, \mathrm{AC}\}$).
Output: The updated cost matrix C.

if $R = R1$ **then return** C
if $R = R2$ **then**
    $uterm \leftarrow M$
else
    $uterm \leftarrow M \times r$
for $n \leftarrow 1$, $\mathrm{len}(L) - 1$ **do**
    $C(L(n), L(n+1)) \leftarrow C(L(n), L(n+1)) + uterm$
    $C(L(n+1), L(n)) \leftarrow C(L(n+1), L(n)) + uterm$
return C

B. Dynamic Routing in the Optical Layer

The physical-layer agility provided by SDN control is an effective solution to the problem of cascading failures in software-defined optical transmission systems. Although the cyber-physical interdependency between the IP control network and physical fiber network results in cascading failure events due to the disconnection of nodes from the network controller, the synergistic operation of the control and data plane entities holds promise for high network survivability [28]. Dynamic routing in the optical layer using intelligent SDN control is actually an example of optical layer restoration. The idea is to reroute connections around the points of failure as much as possible. In an optical C-RAN comprising control, fronthaul, and backhaul connections, the failure propagation and connection restoration mechanisms follow the sequence in the list below. The failure event is assumed to be initiated by a single ROADM node failure.

1) With a node failure, all fibers connected to that node also fail and a new physical fiber topology is formed.
2) Any connection originating or terminating at the failed node also fails. If a fronthaul (backhaul) connection fails, its corresponding backhaul (fronthaul) connection also fails.
3) The remaining connections that have been affected by the node failure could survive if they can be mapped onto another route with available capacity. Nevertheless, if the rerouting of a connection violates the service requirements (e.g., due to the limited end-to-end fronthaul latency), the connection should be dropped.
4) As a result of the failure, the control plane logical topology gets updated. If any node loses connection to the BBH hub, it will also fail.
5) The failure cascade terminates when no new node loses connection to the controller at the end of an iteration.

Order of Events with Dynamic Routing

Inputs: F : failure trigger index; B : BBH hub index (i.e., the location of the SDN controller); C : physical fiber-network topology matrix; CP : logical control-plane topology matrix; SC : set of all connections including their attributes and routes.

$SF \leftarrow \{F\}$ ▷ set of future failing nodes
while $SF \neq \emptyset$ **do**
    Let f denote the index of the upcoming failing node
    $C(f, :) \leftarrow 0$
    $C(:, f) \leftarrow 0$ ▷ All fibers connected to f fail
    for any connection c in SC affected by f **do**
        if $\mathrm{src}(c) = f$ **or** $\mathrm{dst}(c) = f$ **then**
            $SC \leftarrow SC - c$ ▷ c fails and is removed
            if c is a backhaul(fronthaul) connection **then**
                Its counterpart is removed from SC
            else
                $CP(\mathrm{src}(c), \mathrm{dst}(c)) \leftarrow 0$
                $CP(\mathrm{dst}(c), \mathrm{src}(c)) \leftarrow 0$
        else if c can be rerouted **and** satisfy latency **then**
            Update the information for c in SC
        else
            $SC \leftarrow SC - c$
            if c is an X-haul connection **then**
                Its counterpart is removed from SC
            else
                $CP(\mathrm{src}(c), \mathrm{dst}(c)) \leftarrow 0$
                $CP(\mathrm{dst}(c), \mathrm{src}(c)) \leftarrow 0$
    for any operating node n **do**
        if n cannot reach B using the updated CP **then**
            Add n to SF as a next step failing node

The chart above shows the order of events with dynamic

routing when a failure takes place at node F. According to the pseudocode, if a failing connection is a control plane connection, then the control plane matrix, CP, is updated upon the removal of that connection. However, if the failing connection is a fronthaul (backhaul) connection, then it is simply removed along with its corresponding backhaul (fronthaul) connection (leaving CP unchanged). Compared to the load balancing technique, dynamic routing relies on fast network reconfiguration capability. In this paper, we study the two proposed mechanisms independently as well as jointly in terms of effectiveness for reliable optical C-RAN operation.

IV. Results and Discussion

To study the impact of the optical-layer routing mechanisms on the C-RAN failure response, we consider two physical fiber topologies. Fig. 3(a) depicts the 24-node U.S. topology with 43 bidirectional links (average node degree: 3.6), and Fig. 3(b) depicts the 28-node pan-E.U. topology with 41 bidirectional links (average node degree: 2.9). Please note that while these topologies pertain to long-haul networks, we adopt them in our analysis by assuming that fiber lengths have been properly scaled down to satisfy the fronthaul latency constraints. In the given topologies, each ROADM node is connected to one MBS and 10 SCBSs. An SCBS is assumed to be active with probability 0.5. In each network one node serves as the BBH hub and another as the EPC hub. In order to take into account the fronthaul segment latency constraints, we pick the BBH hub as the node with the minimum average distance to every other node in the network. Considering d_{ij} to denote the minimum hop-count distance of node j from node i in an N-node network, we define D_i to be the average distance of node i and calculate it as

$$\mathrm{D}_i = \frac{1}{N-1} \sum_{j=1, j\neq i}^{N} \mathrm{d}_{ij}. \tag{1}$$

We pick the BBH hub to be located at the position that minimizes (1). In the two proposed topologies,

$$\mathrm{D}_{i,min} = \begin{cases} 2.22\,|_{i=9} & \text{(24-node)} \\ 2.67\,|_{i=19} & \text{(28-node)} \end{cases}. \tag{2}$$

The considered BBH hub locations are naturally central in the topologies and point to nodes of higher degrees. Due to space constraints, we only report our results for the EPC hub location that makes the network most vulnerable under static optical layer operation. We consider the aggregation coefficient, AC, to be equal to 10 [26]. In our analysis, the logical control plane is implemented as a uniformly randomly generated connected graph that comprises 10% of the total number of links in a full mesh topology. We use shortest-path routing (as described in Section III) with first-fit wavelength assignment (with 96 available wavelengths) for mapping control plane, fronthaul, and backhaul connections onto the physical fiber network.

To examine the optical C-RAN survivability, we induce a node failure at a certain location (i.e., failure trigger location) and study the failure cascade in the system. we define two quantities: 1) Optical network survival percentage (optical NSP), and 2) wireless network survival percentage (wireless NSP). NSP is defined as the percentage of the surviving nodes at the end of the failure event divided by the number of nodes that can fail in the network. As for the optical network with N ROADM nodes, the number of nodes that can fail is $N-1$ since the BBH hub is assumed to be highly protected. In the heterogeneous wireless network, wireless NSP is the percentage of the number of active RRHs at the end of the failure cascade to the number of initially active RRHs.

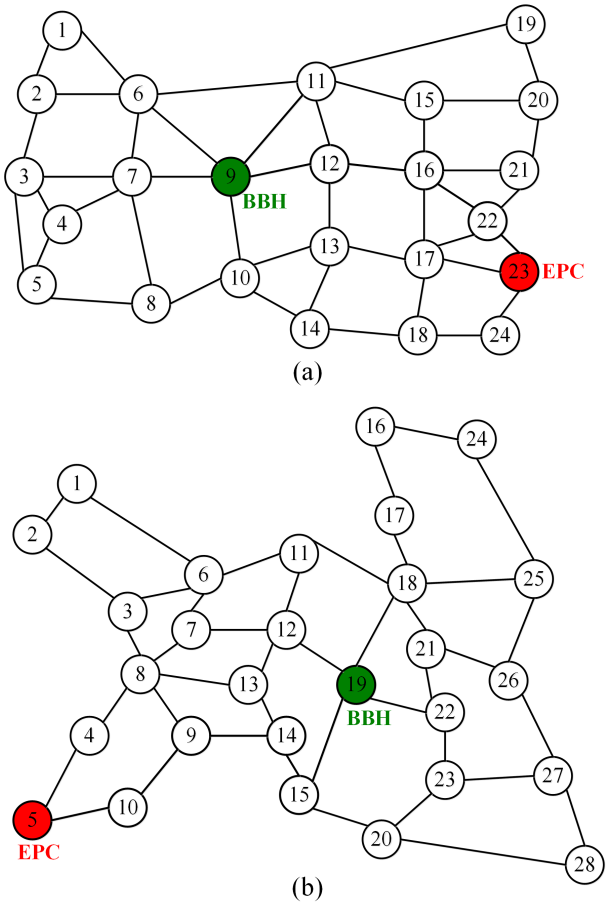

Fig. 3: Optical X-haul topologies: (a) 24-node U.S. network, (b) 28-node E.U. network.

To report any data point, we average the results over 1,000 Monte Carlo simulation runs and also include 95% confidence intervals (CIs). The CIs are calculated using the method of batch means with 50 batches of 20 samples [45, ch 8]. We examine our results in two different subsections, pertaining to the distinct roles of optical-layer load balancing and agility.

A. Load Balancing Impact

Fig. 4 depicts the optical and wireless NSP versus failure trigger location for a fixed set of BBH and EPC hubs, considering the three routing mechanisms of Sec. III. Here, the physical layer is assumed to be static to study the load balancing impact in isolation. With R1 (minimum hop-count routing), according to Fig. 4(c), the wireless NSP in the 24-node network averaged

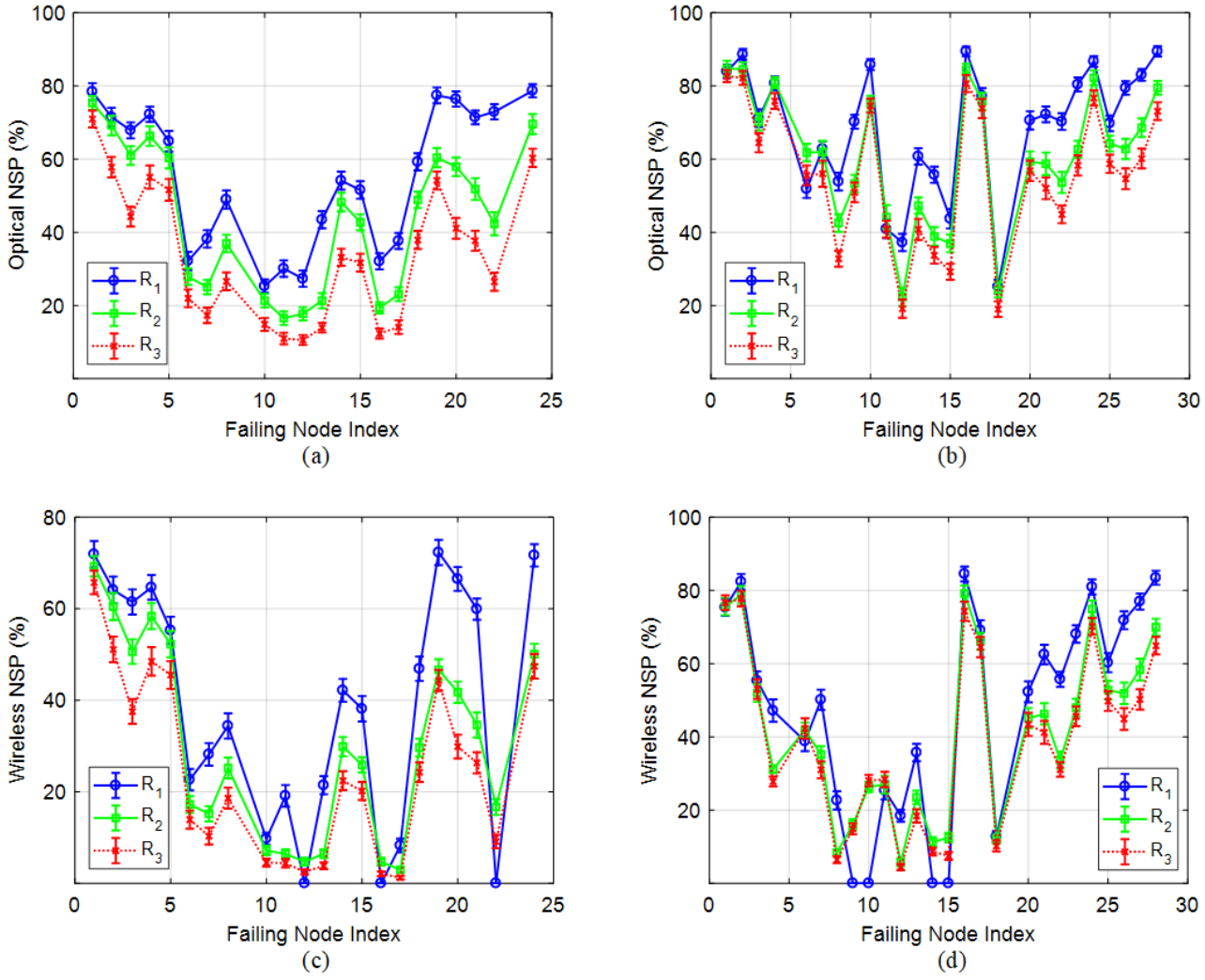

Fig. 4: Optical network survival percentage versus failure trigger location under different routing strategies for (a) 24-node U.S and (b) 28-node E.U. topologies. Wireless network survival percentage versus failure trigger location for (c) 24-node U.S. and (d) 28-node E.U. topologies.

over 22 possible failure trigger locations (excluding the BBH and EPC hubs as in Fig. 3(a)) is 39%. This is the minimum average wireless NSP that can be achieved as a function of the EPC hub location. If we keep the BBH hub location fixed and move the EPC hub to node 10, then the wireless NSP (averaged over possible failure trigger locations) achieves its maximum value (i.e., 54%). Averaging over all possible EPC hub and failure trigger locations, a value of 47.5% can be achieved. As for the 28-node topology, the wireless NSP averaged over 27 possible EPC hub locations (excluding the BBH hub fixed @ node 19) is 59.4% (minimum: 47.3% with EPC hub @ node 5 as in Figs. 3(b) and 4(d), maximum: 67% with EPC hub @ node 18). In general, the further apart the BBH and EPC hubs, the more vulnerable the C-RAN.

Considering the optical X-haul network alone, failure at high-degree nodes generally results in longer failure cascades due to the cyber-physical interdependency between the IP control and physical fiber networks. Interestingly, the use of load balancing (routing strategies R2 and R3) does not improve the optical system robustness. The average 24-node optical NSP is equal to 55.1% for R1, 43.8% for R2, and only 33.9% for R3. In the 28-node optical network, these values are equal to 68.5%, 60.8%, and 55.7%, respectively.

Considering Figs. 4(c) and 4(d), the failure response of the wireless network closely follows that of the optical X-haul network except when a failure in the backhaul segment results in a total network outage. With R1, no load balancing takes place and the low-capacity backhaul connections get aggregated onto a critical path connecting the BBH and EPC hubs. In Fig. 3(a) the critical backhaul path includes nodes 9, 12, 16, 22, and 23. In Fig. 3(b) this route includes nodes 19, 15, 14, 9, 10, and 5. While a failure at such node locations leads to total wireless network failure with R1, load balancing results in marginal improvement. Overall, the survival rate in the wireless network is smaller than that of the optical network. The average wireless NSP is 39% for R1, 29.8% for R2, and 24.3% for R3 in the U.S. topology. In the E.U. topology, these values are equal to 47.3%, 41.7%, and 39.1%, respectively. This degraded performance is primarily due to the fact that two connections (i.e., fronthaul and backhaul) need to be active for

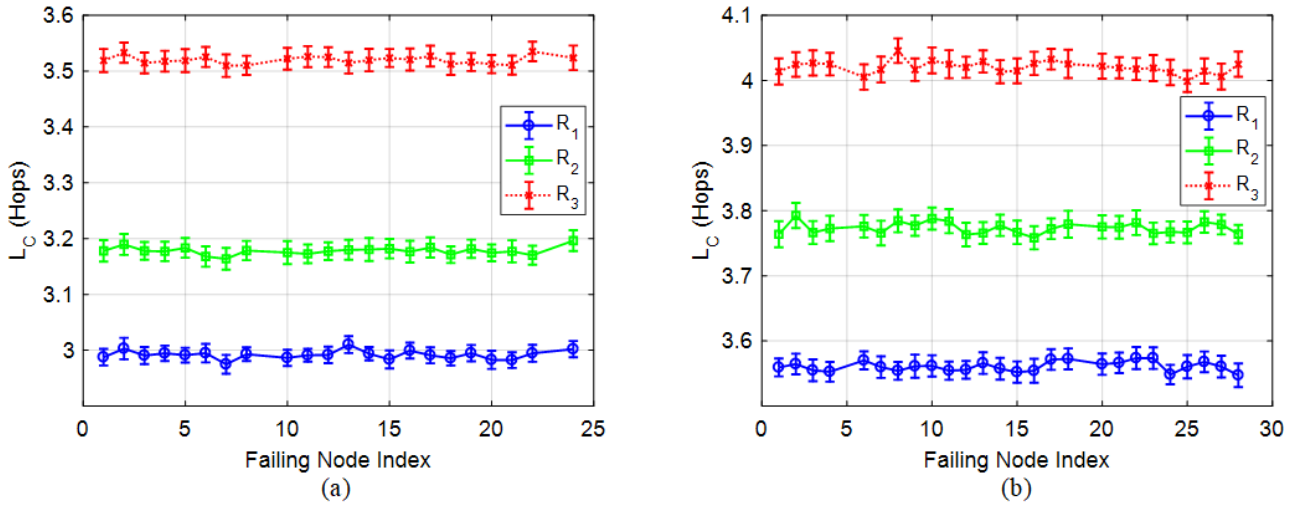

Fig. 5: Average control plane connection hop count vs. failing node index considering different routing strategies for (a) 24-node U.S and (b) 28-node E.U. topologies.

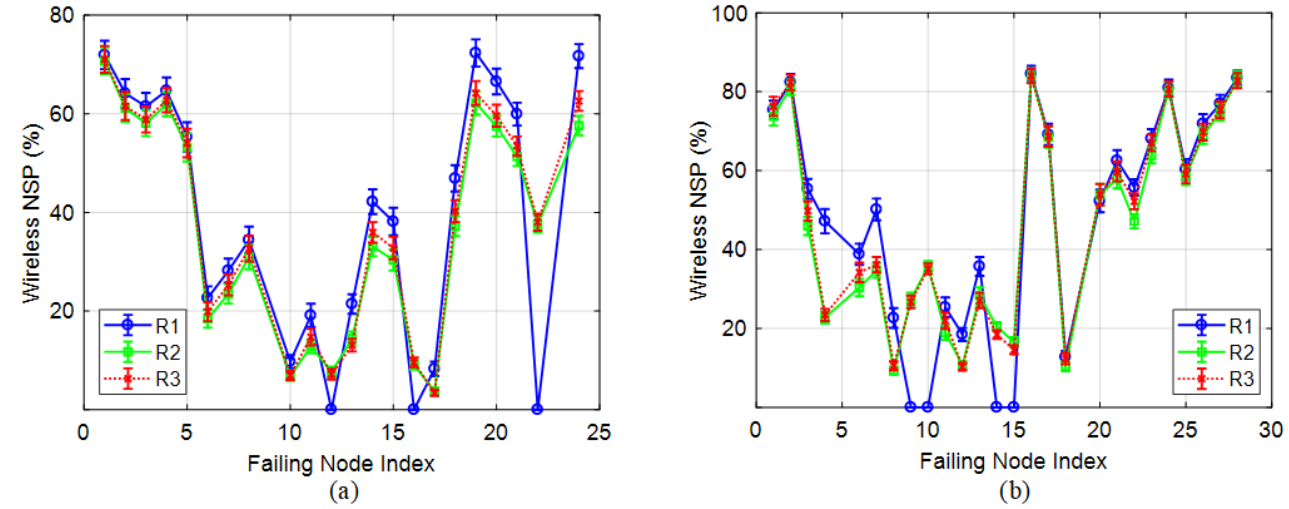

Fig. 6: Wireless network survival percentage versus failure trigger location for (a) 24-node U.S and (b) 28-node E.U. topologies (without load balancing in the control plane).

any wireless network node to survive, whereas in the optical network a node should only be somehow connected to the SDN controller.

To understand the negligible and in some sense the detrimental impact of load-balanced routing, we investigate the properties of the control plane. Fig. 5 depicts the average SDN control plane connection length, L_{C}, based on the three routing mechanisms. Considering that the connections are generated randomly with uniform distribution in a network of N nodes, L_{C} can be expressed as

$$L_{\mathrm{C}} = \frac{1}{N^2 - N} \sum_{i=1}^{N} \sum_{j=1, j \neq i}^{N} \mathrm{d}_{ij}. \tag{3}$$

With R1, it is easy to theoretically calculate L_{C}. In the U.S. network, L_{C}=2.99 hops. In the E.U. network, L_{C}=3.56 hops. These values are in agreement with the values achieved via simulations. With load balancing, L_{C} should naturally grow as the cost matrix becomes dynamic and minimum-hop count routing is no longer in place. With R2, L_{C}=3.18 hops in the U.S. network and 3.77 hops in the E.U. network. With R3, L_{C}=3.52 hops in the U.S. network and 4.02 hops in the E.U. network. In fact, the increased control plane connection lengths due to load balancing account for the increased vulnerability of the optical C-RAN. Longer connections are more correlated and less path disjoint, hence more vulnerable to node failures [46].

Fig. 6 depicts the impact of load balancing when the control and data planes are treated differently. In this scenario, the control plane connections are first routed using R1 (no load balancing) and then the fronthaul and backhaul connections are routed based on R1, R2, or R3. In other words, load

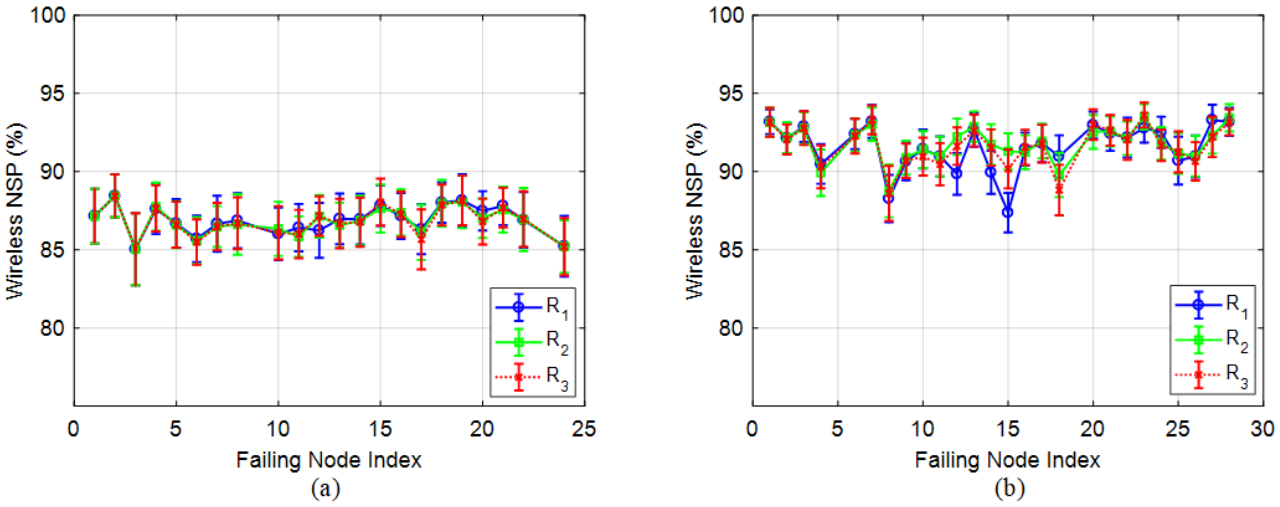

Fig. 7: Interplay of dynamic routing and load balancing in (a) 24-node U.S and (b) 28-node E.U. topologies.

balancing is only applied to the data plane to prevent the undesired increase in L_{C}. With this isolation the failure response is slightly improved (better minimum NSP without compromising the overall performance), but not so much so that the network can be considered failure resilient. As a soft mechanism, load balancing is expected to be more effective for the case of fiber cuts within a soft failure framework. It is not strong enough to counteract hard node failures leading to multiple simultaneous fiber cuts.

B. Dynamic Routing Impact

While load balancing alone could not significantly improve the survivability of the software-defined optical C-RAN, in this section we look at the potential gains of physical layer agility (as elaborated in Section III-B), taking into account the fronthaul latency constraints. Previous work has demonstrated the benefits of dynamic routing in software-defined optical transmission networks [28], [46]. Here, we only report our results for the RAN segment.

Fig. 7 depicts the wireless NSP versus initial node failure index for the U.S. and E.U. topologies and the three routing mechanisms. A progammable X-haul network significantly improves the RAN robustness by rerouting control plane as well as fronthaul and backhaul connections around the points of failure, irrespective of the routing strategy involved. With an agile optical layer, the average wireless NSP in the U.S. network is equal to 86.9% with R1, 86.8% with R2, and 86.8% with R3. In the E.U. network, these values are respectively equal to 91.6%, 91.8%, and 91.7%. Note that a portion of the wireless network failures are enforced by the failure trigger event. The RRHs connected to the ROADM node failing in the first place cannot be saved.

As the choice of routing cost matrix does not matter with a dynamic X-haul network, we report the rest of our results under R2. Since the modification of the physical fiber topology and the rerouting of connections result in increased connection lengths, the increased latency in the fronthaul segment, as a highly latency-sensitive segment of the network, should be taken into account. In Fig. 8, we report average fronthaul hop count, L_{F}, versus failure trigger location either before or after the failure events. With R1, the average fronthaul connection hop count in the U.S. network is $\mathrm{D}_9 = 2.22$ hops. This value is $\mathrm{D}_{19} = 2.67$ hops in the E.U. network. With R2, the connection lengths are longer and $L_{\mathrm{F}} = 2.53$ hops in the U.S. network and 2.93 hops in the E.U. network. The rerouting of connections upon failure does not lead to a significant increase of L_{F}. The average increase is equal to 2.3% and 1.87% in the U.S. and E.U. topologies, respectively. Typically the failure events triggered at the nodes neighboring the BBH hub result in the most significant impact. In the U.S. network, the maximum increase in L_{F} is realized when the initial failure takes place at node 7 (hop count increase: 10.6%). In the E.U. network, the failure at node 18 leads to the maximum increase in latency (15.3%).

Finally, we study the wireless network survivability performance when the maximum fronthaul hop count, $\mathrm{H}_{\max}$, is capped by a hard limit. According to Fig. 3, in the U.S. topology the BBH hub can reach any other node in less than 5 hops (i.e., $\mathrm{H}_{\max} = 4$). As well, in the E.U. topology, $\mathrm{H}_{\max} = 5$. The results in Fig. 9 imply that even without changing the maximum fronhaul hop count limit, the dynamic routing of connections can result in a very high wireless NSP. In the U.S. network, the minimum (mean) wireless NSP is 79.3% (84.7%) for $\mathrm{H}_{\max} = 4$ and saturates at 85% (86.8%) for $\mathrm{H}_{\max} = \infty$. On the other hand, in the E.U. network, the minimum (mean) wireless NSP varies between 81.7% (89.8%) for $\mathrm{H}_{\max} = 5$ and 88.8% (91.8%) for $\mathrm{H}_{\max} = \infty$.

V. Conclusion

The proliferation of 5G C-RAN architectures employing a software-defined reconfigurable optical transport network calls for the reliability assessment of such systems within the context of network dependencies. In this paper, we studied the impact of optical-layer load balancing and infrastructure

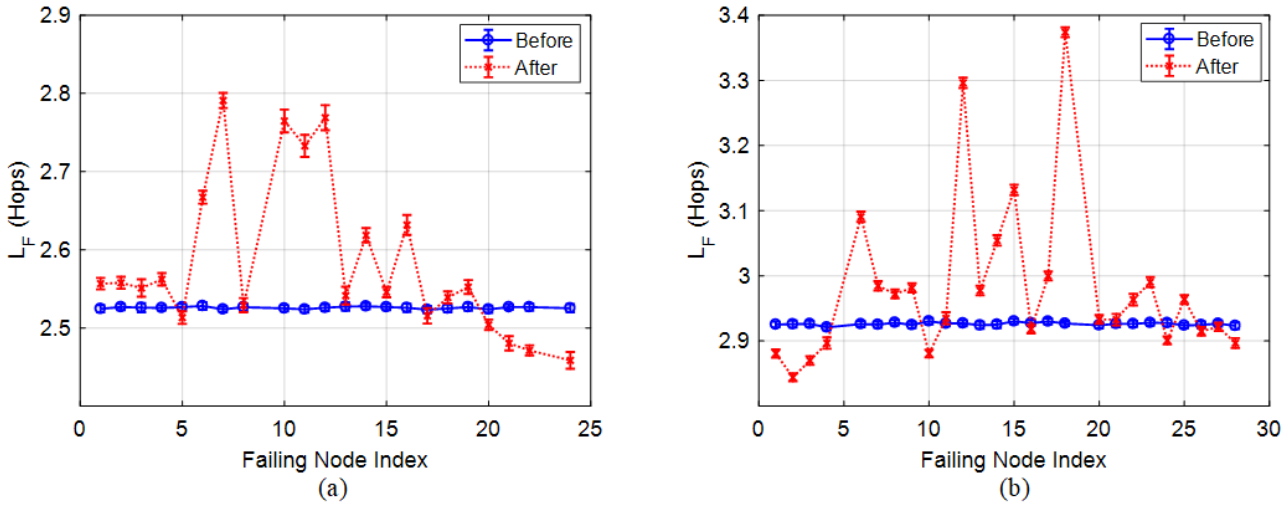

Fig. 8: Average fronthaul connection hop count versus failure trigger location under R_2 for (a) 24-node U.S and (b) 28-node E.U. topologies.

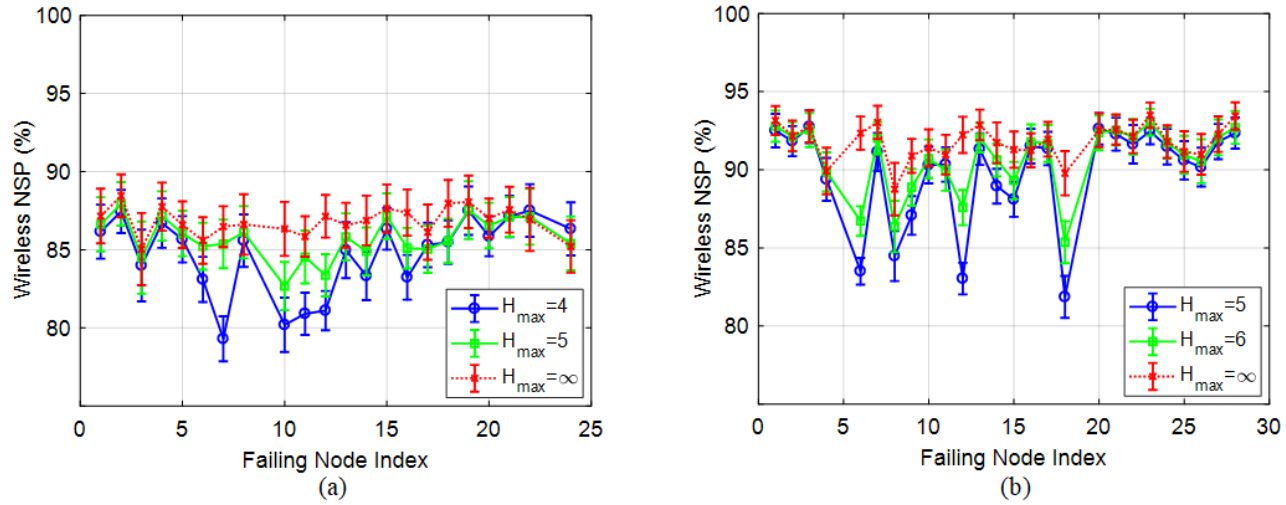

Fig. 9: Impact of maximum permissible fronthaul connection length on wireless network survival percentage in (a) 24-node U.S and (b) 28-node E.U. topologies.

programmability on the survivability of a software-defined C-RAN, taking into account the three-way dependencies among the optical, radio, and higher-layer control entities. Under a hard node failure model, load balancing could barely prevent a total wireless network outage state by distributing connections. With load balancing, the best minimum RAN survival percentage was 3.8% in the 24-node U.S. network and 10.2% in the 28-node pan-E.U. network. These values could be achieved by isolating the routing in the control and data planes. A control plane topology employing load balancing was found to be detrimental as longer connections result in larger failure cascades in the optical X-haul network.

Unlike load balancing, X-haul network infrastructure programmability proved to be a strong means for achieving significantly robust C-RAN operation with no sensitivity to critical network elements. Our analysis indicated that the impact of reconfiguration on the latency-sensitive fronthaul segment is negligible, with the penalty being strongest when the failure event is triggered at a BBH hub's neighboring node. While the choice of BBH and EPC hub location did not have a significant impact on C-RAN reliability with X-haul reconfiguration, future work should consider the case of multiple BBH and EPC hubs in the network in order to examine the trade-offs between statistical multiplexing and reliability gains due to resource redundancies. Furthermore, due to the heterogeneous nature of C-RANs, it will be instrumental to study their survivability based on a hybrid X-haul network, comprising various link types (e.g., fiber, free space optical) with different failure probabilities.

ACKNOWLEDGMENT

This work was supported by the Natural Sciences and Engineering Research Council of Canada (NSERC) and the

NSF Center for Integrated Access Networks (CIAN) under grant no. EEC-0812072.

REFERENCES

[1] P. Iovanna, F. Cavaliere, F. Testa, S. Stracca, G. Bottari, F. Ponzini, A. Bianchi, and R. Sabella, "Future proof optical network infrastructure for 5G transport," *IEEE J. Opt. Commun. Netw.*, vol. 8, no. 12, pp. B80–B92, Dec. 2016.

[2] M. Ruffini, M. Achouche, A. Arbelaez, R. Bonk, A. D. Giglio, N. J. Doran, M. Furdek, R. Jensen, J. Montalvo, N. Parsons, T. Pfeiffer, L. Quesada, C. Raack, H. Rohde, M. Schiano, G. Talli, P. Townsend, P. Wessaly, L. Wosinska, X. Yin, and D. B. Payne, "Access and metro network convergence for flexible end-to-end network design," *IEEE J. Opt. Commun. Netw.*, vol. 9, no. 6, pp. 524–535, Jun. 2017.

[3] A. Tzanakaki, M. Anastasopoulos, I. Berberana, D. Syrivelis, P. Flegkas, T. Korakis, D. Camps-Mur, I. Demirkol, J. Gutiérrez, E. Grass, Q. Wei, E. Pateromichelakis, N. Vucic, A. Fehske, M. Grieger, M. Eiselt, J. Bartelt, G. Fettweis, G. Lyberopoulos, E. Theodoropoulou, and D. Simeonidou, "Wireless-optical network convergence: enabling the 5G architecture to support operational and end-user services," *IEEE Commun. Mag.*, vol. 55, no. 10, pp. 184–192, Oct. 2017.

[4] M. Fiorani, S. Tombaz, J. Mårtensson, B. Skubic, L. Wosinska, and P. Monti, "Modeling energy performance of C-RAN with optical transport in 5G network scenarios," *IEEE J. Opt. Commun. Netw.*, vol. 8, no. 11, pp. B21–B34, Nov. 2016.

[5] P. K. Agyapong, M. Iwamura, D. Staehle, W. Kiess, and A. Benjebbour, "Design considerations for a 5G network architecture," *IEEE Commun. Mag.*, vol. 52, no. 11, pp. 65–75, Nov. 2014.

[6] N. Wang, E. Hossain, and V. K. Bhargava, "Backhauling 5G small cells: a radio resource management perspective," *IEEE Wireless Communications*, vol. 22, no. 5, pp. 41–49, Oct. 2015.

[7] X. Wang, C. Cavdar, L. Wang, M. Tornatore, H. S. Chung, H. H. Lee, S. M. Park, and B. Mukherjee, "Virtualized cloud radio access network for 5G transport," *IEEE Commun. Mag.*, vol. 55, no. 9, pp. 202–209, Sep. 2017.

[8] M. R. Raza, M. Fiorani, A. Rostami, P. Öhlen, L. Wosinska, and P. Monti, "Dynamic slicing approach for multi-tenant 5G transport networks," *IEEE J. Opt. Commun. Netw.*, vol. 10, no. 1, pp. A77–A90, Jan. 2018.

[9] F. Z. Yousaf, M. Bredel, S. Schaller, and F. Schneider, "NFV and SDN–key technology enablers for 5G networks," *IEEE J. Sel. Areas Commun.*, vol. 35, no. 11, pp. 2468–2478, Nov. 2017.

[10] J. Liu, M. Sheng, L. Liu, and J. Li, "Network densification in 5G: from the short-range communications perspective," *IEEE Commun. Mag.*, vol. 55, no. 12, pp. 96–102, Dec. 2017.

[11] T. Biermann, L. Scalia, C. Choi, W. Kellerer, and H. Karl, "How backhaul networks influence the feasibility of coordinated multipoint in cellular networks," *IIEEE Commun. Mag.*, vol. 51, no. 8, pp. 168–176, Aug. 2013.

[12] M. R. Raza, M. Fiorani, A. Rostami, P. Öhlén, L. Wosinska, and P. Monti, "Demonstration of dynamic resource sharing benefits in an optical C-RAN," *IEEE J. Opt. Commun. Netw.*, vol. 8, no. 8, pp. 621–632, Aug. 2016.

[13] T. Pfeiffer, "Next generation mobile fronthaul and midhaul architectures," *IEEE J. Opt. Commun. Netw.*, vol. 7, no. 11, pp. B38–B45, Nov. 2015.

[14] X. Liu and F. Effenberger, "Emerging optical access network technologies for 5G Wireless," *IEEE J. Opt. Commun. Netw.*, vol. 8, no. 12, pp. B70–B79, Dec. 2016.

[15] K. Zhang, Q. Zhuge, H. Xin, H. He, W. Hu, and D. V. Plant, "Low-cost WDM fronthaul enabled by partitioned asymmetric AWGR with simultaneous flexible transceiver assignment and chirp management," *IEEE J. Opt. Commun. Netw.*, vol. 9, no. 10, pp. 876–888, Oct. 2017.

[16] J. Zhang, Y. Ji, S. Jia, H. Li, X. Yu, and X. Wang, "Reconfigurable optical mobile fronthaul networks for coordinated multipoint transmission and reception in 5G," *IEEE J. Opt. Commun. Netw.*, vol. 9, no. 6, pp. 489–497, Jun. 2017.

[17] P. Chanclou, L. A. Neto, K. Grzybowski, Z. Tayq, F. Saliou, and N. Genay, "Mobile fronthaul architecture and technologies: a RAN equipment assessment," *IEEE J. Opt. Commun. Netw.*, vol. 10, no. 1, pp. A1–A7, Jan. 2018.

[18] S. Zhou, X. Liu, F. Effenberger, and J. Chao, "Low-latency high-efficiency mobile fronthaul with TDM-PON (mobile-PON)," *IEEE J. Opt. Commun. Netw.*, vol. 10, no. 1, pp. A20–A26, Jan. 2018.

[19] L. Velasco, A. Castro, A. Asensio, M. Ruiz, G. Liu, C. Qin, R. Proietti, and S. J. B. Yoo, "Meeting the requirements to deploy cloud RAN over optical networks," *IEEE J. Opt. Commun. Netw.*, vol. 9, no. 3, pp. B22–B32, Mar. 2017.

[20] A. S. Gowda, L. G. Kazovsky, K. Wang, and D. Larrabeiti, "Quasi-passive optical infrastructure for future 5G wireless networks: pros and cons," *IEEE J. Opt. Commun. Netw.*, vol. 8, no. 12, pp. B111–B123, Dec. 2016.

[21] M. Channegowda, R. Nejabati, and D. Simeonidou, "Software-defined optical networks technology and infrastructure: enabling software-defined optical network operations," *IEEE J. Opt. Commun. Netw.*, vol. 5, no. 10, pp. A274–A282, Oct. 2013.

[22] S. Gringeri, N. Bitar, and T. J. Xia, "Extending software defined network principles to include optical transport," *IEEE Commun. Mag.*, vol. 51, no. 3, pp. 32–40, Mar. 2013.

[23] R. Alvizu, G. Maier, N. Kukreja, A. Pattavina, R. Morro, A. Capello, and C. Cavazzoni, "Comprehensive survey on T-SDN: software-defined networking for transport networks," *Commun. Surveys Tuts.*, vol. 19, no. 4, pp. 2232–2283, Fourth Quarter 2017.

[24] J. S. Choi, "Hierarchical distributed orchestration framework for multi-domain SDTNs," *IEEE J. Opt. Commun. Netw.*, vol. 9, no. 12, pp. 1125–1135, Dec. 2017.

[25] Z. Cheng, X. Zhang, Y. Li, S. Yu, R. Lin, and L. He, "Congestion-aware local reroute for fast failure recovery in software-defined networks," *IEEE J. Opt. Commun. Netw.*, vol. 9, no. 11, pp. 934–944, Nov. 2017.

[26] M. Fiorani, A. Rostami, L. Wosinska, and P. Monti, "Abstraction models for optical 5G transport networks," *IEEE J. Opt. Commun. Netw.*, vol. 8, no. 9, pp. 656–665, Sep. 2016.

[27] P. Öhlén, B. Skubic, A. Rostami, M. Fiorani, P. Monti, Z. Ghebretensaé, J. Mårtensson, K. Wang, and L. Wosinska, "Data plane and control architectures for 5G transport networks," *J. Lightw. Technol.*, vol. 34, no. 6, pp. 1501–1508, Mar. 2016.

[28] H. Rastegarfar, D. C. Kilper, M. Glick, and N. Peyghambarian, "Cyber-physical interdependency in dynamic software-defined optical transmission networks," *IEEE J. Opt. Commun. Netw.*, vol. 7, no. 12, pp. 1126–1134, Dec. 2015.

[29] M. Parandehgheibi, E. Modiano, and D. Hay, "Mitigating cascading failures in interdependent power grids and communication networks," in *2014 IEEE International Conference on Smart Grid Communications (SmartGridComm)*, Nov. 2014, pp. 242–247.

[30] M. Parandehgheibi and E. Modiano, "Robustness of interdependent networks: the case of communication networks and the power grid," in *2013 IEEE Global Communications Conference (GLOBECOM)*, Dec. 2013, pp. 2164–2169.

[31] M. Parandehgheibi, H.-W. Lee, and E. Modiano, "Survivable path sets: a new approach to survivability in multilayer networks," *J. Lightw. Technol.*, vol. 32, no. 24, pp. 4139–4150, Dec. 2014.

[32] M. F. Habib, M. Tornatore, and B. Mukherjee, "Cascading-failure-resilient interconnection for interdependent power grid-optical networks," in *Optical Fiber Communications Conference and Exhibition (OFC)*, Mar. 2015, p. M3I.3.

[33] S. Chattopadhyay, H. Dai, D. Y. Eun, and S. Hosseinalipour, "Designing optimal interlink patterns to maximize robustness of interdependent networks against cascading failures," *IEEE Trans. Commun.*, vol. 65, no. 9, pp. 3847–3862, Sep. 2017.

[34] Z. Mayer, J. Li, A. Papadogiannis, and T. Svensson, "On the impact of control channel reliability on coordinated multi-point transmission," *EURASIP Journal on Wireless Communications and Networking*, vol. 2014, no. 28, pp. 1–16, Dec. 2014.

[35] I. A. Alimi, A. L. Teixeira, and P. P. Monteiro, "Toward an efficient C-RAN optical fronthaul for the future networks: a tutorial on technologies, requirements, challenges, and solutions," *Commun. Surveys Tuts.*, vol. 20, no. 1, pp. 708–769, First Quarter 2018.

[36] H. Beyranvand, M. Lévesque, M. Maier, J. A. Salehi, C. Verikoukis, and D. Tipper, "Toward 5G: FiWi enhanced LTE-A HetNets with reliable low-latency fiber backhaul sharing and WiFi offloading," *IEEE/ACM Trans. Netw.*, vol. 25, no. 2, pp. 690–707, Apr. 2017.

[37] E. Wong, E. Grigoreva, L. Wosinska, and C. M. Machuca, "Enhancing the survivability and power savings of 5G transport networks based on DWDM rings," *IEEE J. Opt. Commun. Netw.*, vol. 9, no. 9, pp. D74–D85, Sep. 2017.

[38] H. Rastegarfar, T. Svensson, and N. Peyghambarian, "Reliability gains of infrastructure programmability in an optical C-RAN," in *Optical Fiber Communications Conference and Exhibition (OFC)*, Mar. 2018, p. Th2A.40.

[39] P. Wang, H. Xu, L. Huang, J. He, and Z. Meng, "Control link load balancing and low delay route deployment for software defined networks," *IEEE J. Sel. Areas Commun.*, vol. 35, no. 11, pp. 2446–2456, Nov. 2017.
[40] H. Li, P. Li, S. Guo, and A. Nayak, "Byzantine-resilient secure software-defined networks with multiple controllers in cloud," *IEEE Transactions on Cloud Computing*, vol. 2, no. 4, pp. 436–447, Oct.-Dec. 2014.
[41] X. Chen, B. Zhao, S. Ma, C. Chen, D. Hu, W. Zhou, and Z. Zhu, "Leveraging master-slave OpenFlow controller arrangement to improve control plane resiliency in SD-EONs," *Optics Express*, vol. 23, no. 6, pp. 7550–7558, Mar. 2015.
[42] V. Sridharan, M. Gurusamy, and T. Truong-Huu, "On multiple controller mapping in software defined networks with resilience constraints," *IEEE Commun. Lett.*, vol. 21, no. 8, pp. 1763–1766, Aug. 2017.
[43] P. C. R. Fonseca and E. S. Mota, "A survey on fault management in software-defined networks," *Commun. Surveys Tuts.*, vol. 19, no. 4, pp. 2284–2321, Fourth Quarter 2017.
[44] H. Rastegarfar, L. A. Rusch, and A. Leon-Garcia, "Optical load-balancing tradeoffs in wavelength-routing cloud data centers," *IEEE J. Opt. Commun. Netw.*, vol. 7, no. 4, pp. 286–300, Apr. 2015.
[45] A. Leon-Garcia, *Probability, Statistics, and Random Processes for Electrical Engineering (3rd Edition)*. Prentice Hall, Upper Saddle River, New Jersey, 2008.
[46] H. Rastegarfar, D. C. Kilper, M. Glick, and N. Peyghambarian, "Topology implications in cyber-physical software-defined optical transmission networks," in *Optical Fiber Communications Conference and Exhibition (OFC)*, Mar. 2016, p. Th4G.1.